Research Square

Preprints are preliminary reports that have not undergone peer review.
They should not be considered conclusive, used to inform clinical practice,
or referenced by the media as validated information.

Spatial Distribution of Size-Resolved Particulate Matter and Associated Heavy Metal Health Risks in a Tier-2 Indian City During Winter

PALANISWAMY VIVEKANANDAN POOJANANDINE

nandhinipooja49@gmail.com

Kumaraguru College of Technology

ARUNACHALAM GANDHIMATHI

Kumaraguru College of Technology

Research Article

Keywords: sources, pm fractions, heavy metals, spatial mapping, health risk

Posted Date: July 8th, 2026

DOI: https://doi.org/10.21203/rs.3.rs-9698656/v1

License: This work is licensed under a Creative Commons Attribution 4.0 International License.
Read Full License

Additional Declarations: No competing interests reported.

Spatial Distribution of Size-Resolved Particulate Matter and Associated Heavy Metal Health Risks in a Tier-2 Indian City During Winter

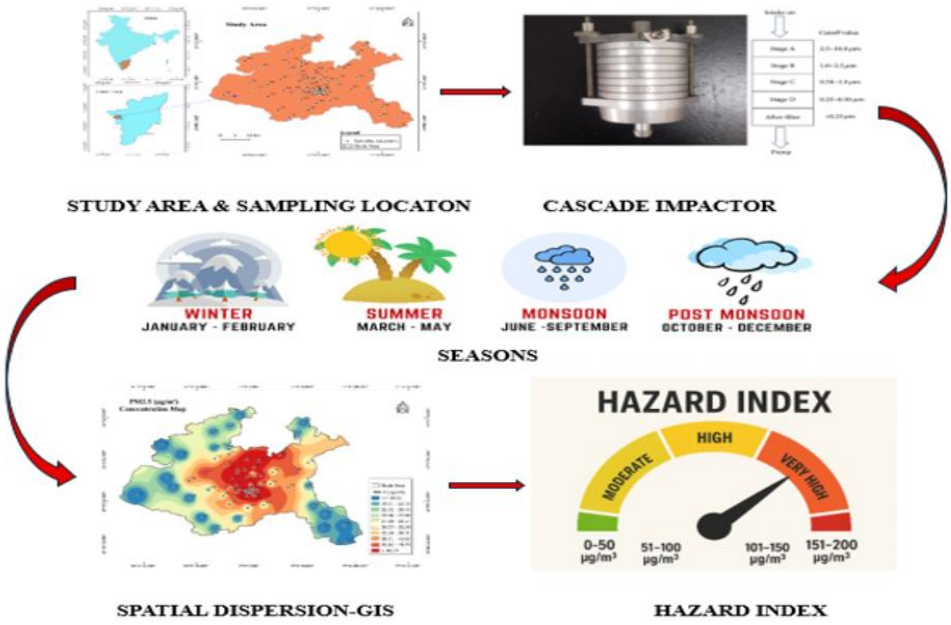
PALANISWAMY VIVEKANANDAN POOJANANDINE[1*], ARUNACHALAM GANDHIMATHI[2]

[1*]Department of Civil Engineering, Kumaraguru College of Technology, Chinnavedampatti, Coimbatore - 641049, Tamil Nadu, India. E-mail: nandhinipooja49@gmail.com

[2]Department of Civil Engineering, Kumaraguru College of Technology, Chinnavedampatti, Coimbatore - 641049, Tamil Nadu, India. E-mail: gandhimathi.a.ce@kct.ac.in

*Corresponding author: nandhinipooja49@gmail.com
Tel: +919486755338

GRAPHICAL ABSTRACT



ABSTRACT

Rapid urbanisation and intensified anthropogenic activities have significantly increased particulate pollution in Indian cities, leading to elevated non-carcinogenic health risks. This study evaluates the spatial distribution of fine and ultrafine particles ($PM_{2.5}$, PM_{1}, $PM_{0.5}$, $PM_{0.25}$, and $<PM_{0.25}$) and $PM_{2.5}$-bound Heavy Metals (HMs) across 70 locations in Coimbatore, covering urban, peri-urban, and rural settlements. $PM_{2.5}$ concentrations ranged from 10.05 to 149.11 μg m^{-3}, with major hotspots observed near the Vellalore dump yard, Chettipalayam, Gandhipuram, and key traffic–industrial corridors. Spatial modelling using IDW identified clear high-exposure zones and pronounced urban–rural gradient. Among the analysed metals, Fe, Zn, and Mn were dominant across all zones, indicating strong contributions from crustal materials and vehicular activity. Toxic metals such as Pb, Cd, As, Cr, and Ni were elevated in landfill and urban regions due to waste burning, industrial emissions, and traffic sources. A consistent trend in metal concentration was observed as: Fe > Zn > Cu > Pb > Cr > Ni > Mn > As > Cd. Strong spatial correspondence between Hazard Index (HI) on $PM_{2.5}$ -bound Heavy Metals (HMs) and $PM_{2.5}$ confirms that fine particles act as carriers of toxic metals, enhancing inhalation risk. The average HI followed: landfill (4.28) > urban (2.96) > peri-urban (1.73) > rural (0.48), with all but rural areas exceeding safe limits. The average life expectancy reduction followed: landfill (9.36 years) > urban (6.86 years) > semi-urban (4.40 years) > rural (0.80 years), indicating a clear gradient of increasing impact with proximity to pollution sources. This study highlights the importance of measuring $PM_{2.5}$, and ultrafine particles and to set standards as they can have severe impact on human population when compared to $PM_{2.5}$ and emphasises the need for improved standard makeup for them with proper waste management techniques, emission control, and continuous monitoring to protect public health.

Keywords: sources; pm fractions; heavy metals; spatial mapping; health risk

INTRODUCTION

Air pollution is a critical and global environmental threat to rapidly urbanising countries on the planet. Adverse health effects and intensified pollution concentration are becoming challenging in developing countries like India due to urban expansion, population growth, industrialization, vehicular explorations and inadequate waste management techniques. Air pollution associates with degradation of other environmental components, including water and soil (Karagulian *et al*., 2015; Manisalidis *et al*., 2020; CPCB, 2022).

90% of the global population is exposed to exceeded $PM_{2.5}$ concentrations according to World Health Organization (WHO) guideline leading to premature mortality (WHO, 2021). In India, particulate matter $PM_{2.5}$ due to anthropogenic activities has bloomed in recent decades and thus pose serious health risks in urban and peri-urban areas (Bont *et al*., 2024). Fine and ultrafine particulate matter ($PM_{2.5}$ and smaller fractions PM_{1}, $PM_{0.5}$, $PM_{0.25}$, and $<PM_{0.25}$) associated with Heavy Metals (HMs) are of particular concern due to their ability to penetrate deep into the lungs, enter systemic circulation, and induce oxidative stress and inflammatory responses affecting multiple organ systems (Xing *et al*., 2016; Gandhimathi *et al*., 2023). Recent studies evident that Heavy Metals (HMs) originating from road dust, soil resuspension, and various anthropogenic activities exhibit a strong affinity for particulate matter. These particles get readily transported through the atmosphere and further aggravate health impacts on human beings (Siudek, 2021; Khan *et al*., 2020).

Ample number of studies has been done on $PM_{2.5}$ and PM_{10}, whereas finer particulate fractions such as PM_{1}, $PM_{0.5}$, $PM_{0.25}$, and $<PM_{0.25}$ has limited attention. This paper has identified a significant research gap, therefore identifying $PM_{2.5}$ and ultrafine particles PM_{1}, $PM_{0.5}$, $PM_{0.25}$, and $<PM_{0.25}$ due to their small size and large surface area. These particles penetrate deep into the alveolar region, translocate into the bloodstream, and pose greater health risks than coarser particles. These particles in association with Heavy Metals (HMs) (As, Cd, Cr, Ni, Pb, Mn, Cu, Zn, and Fe) exhibit higher toxicity, with adverse cardiopulmonary and neurological outcomes and enhanced oxidative potential (Roy *et al*., 2019; Yang *et al*.,2020;WHO,2013;Ali *et al*., 2020; Schraufnagel, 2020; Vallabani *et al*., 2023; Chauhan *et al*.,2024).

Among different seasonality, winter-season has a critical influence on particulate concentrations and intensify population exposure due to lower mixing heights, reduced wind speeds, and stable stratification (Cheng *et al*., 2015).To address this condition seasonal meteorology associated with $PM_{2.5}$, finer fractions of PM_{1}, $PM_{0.5}$, $PM_{0.25}$, and $<PM_{0.25}$ and Heavy Metals (HMs) (As, Cd, Cr, Ni,

Pb, Mn, Cu, Zn, and Fe) were sampled at 70 locations within 30 km radius in and around the study area throughout Jan 2024 – Dec 2024, and subjected to detailed spatial analysis (Sengupta *et al*., 2022;Patra *et al*., 2021; Safarov *et al*., 2024; Hossain *et al*., 2023), using a stratified sampling approach (Morakinyo *et al*., 2021). Special focus on landfill-influenced areas, due to continuous sources of particulate emissions through waste decomposition, dust resuspension, and episodic open burning (Meena *et al*., 2023; Njoku *et al*., 2019; Palmiotto *et al*., 2019).Novelty of the study : (i) To measure the concentration of size-segregated particulate matter ($PM_{2.5}$, PM_{1}, $PM_{0.5}$, $PM_{0.25}$, and $<PM_{0.25}$); (ii) Evaluate meteorological influences on ($PM_{2.5}$, PM_{1}, $PM_{0.5}$, $PM_{0.25}$, and $<PM_{0.25}$); (iii) Analysis of spatial dispersion patterns using GIS for $PM_{2.5}$, PM_{1}, $PM_{0.5}$, $PM_{0.25}$, and $<PM_{0.25}$ and $PM_{2.5}$ - bound HM concentrations ; (iv) Estimate inhalation health risks using Hazard Quotient (HQ) and Hazard Index (HI) due to these particles; and (v) Identify pollution hotspots across the study area.

2. METHODOLOGY

2.1 Description of study area

Coimbatore, locally known as “Kovai,” is a major metropolitan city in Tamil Nadu, India. Covering an area of 4,732 km², Coimbatore comprises 1,628 km² of urban land and 3,104 km² of rural hinterlands (Arunkumar *et al*., 2022). The city on the downwind side of the Western Ghats, remains as a semi-enclosed basin which restricts pollution and pollution concentration to travel throughout the nation due to low wind speed and stable atmospheric condition (Safarov *et al*., 2024).The present study surrounds five taluks of Coimbatore district: Coimbatore North, Coimbatore South, Madukkarai, Sulur, and Perur to ensure representative spatial coverage (Figure 1) and extends up to 30 km for analysing particulate pollution dynamics across diverse land-use categories such as high-traffic urban cores, rapidly expanding peri-urban zones, industrial clusters, and surrounding rural settlements, which has an continuous emission hotspot Vellalore municipal dump yard, thereby capturing urban, peri-urban, and rural environments.

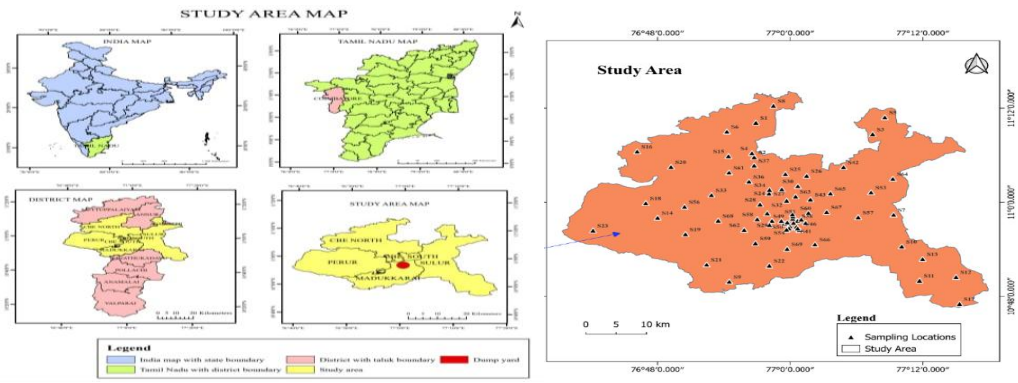


FIG 1. Study area map

2.2 Data Collection and Analysis

Sampling locations were selected using a stratified design based on population density and land-use characteristics, as detailed in Table 1. Settlement classification was derived from Census of India (2011) ward- and village-level data, supplemented with high-resolution gridded population estimates from WorldPop (2023). Locations were categorized as urban, peri-urban, and rural, following established urban transition frameworks reported in Indian and global urbanization studies (SACI, 2023). To better capture transitional emission characteristics and rapid land-use changes, a higher sampling density was assigned to peri-urban zones. (Figure 2) illustrates the spatial distribution of population (2020) and topography (2024) across the study area (WorldPop, 2023).

TABLE 1. Criteria for sampling (Settlement Type ,sources vs. Population Density (Coimbatore, India))

Settlement Type	**Sources**	**Typical Examples (Coimbatore)**	**Population Density (persons km^{-2})**	**Sampling Locations**
Urban	Industrial zones (manufacturing units, textile mills), Major road corridors (high traffic density), Residential areas (high-density housing), Commercial areas (markets, shopping complexes), Mixed-use zones (residential + commercial activities)	Gandhipuram, Peelamedu, Ramanathapuram	>16,000(central municipal wards)	**S24–S37 (14 sites)**
Semi-urban (Peri-urban)	Dump yard / landfill sites, Small-scale industries (workshops, brick kilns), Developing residential layouts, Transport hubs (bus depots, logistics areas), Agricultural–industrial transition zones	Vellalore dump yard, Kuniyamuthur, Sulur, Neelambur	2,000–7,000 (census towns & urban fringes)	**S38–S70 (33 sites)**
Rural	Agricultural fields (crop cultivation areas), Open land / grazing areas,	Anaikatti, Booluvampatti,	<1,000 (typically 400–	**S1–S23 (23 sites)**

	Areas with minimal vehicular activity, Villages with low population density, Forest or green cover areas	Navakkarai, Senjerimalai	800)	

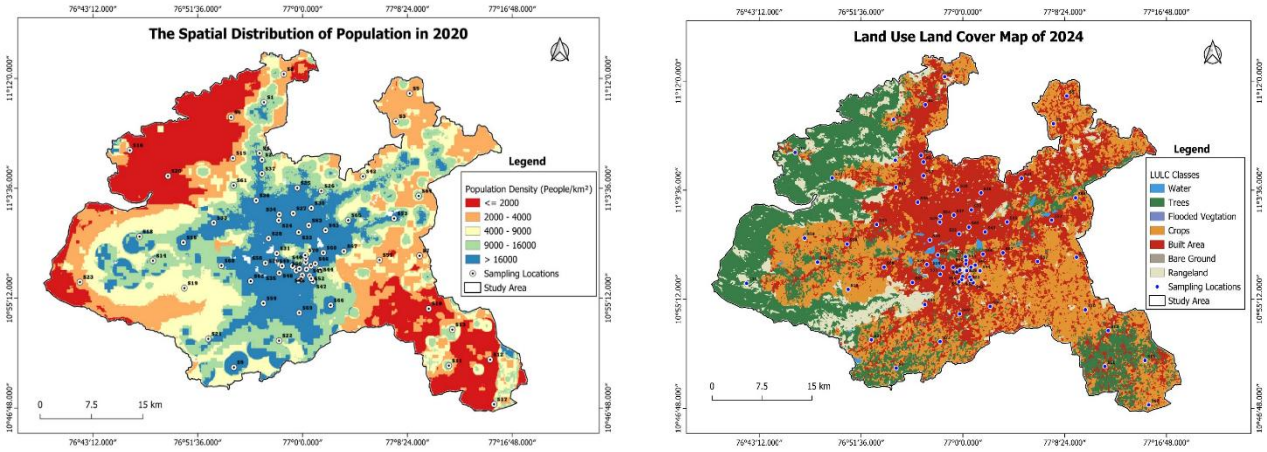


FIG 2. Spatial distribution of population 2020 & topography 2024

2.3 Meteorological Data Acquisition

According to long-term weather trends of western Tamil Nadu, the seasonal data were classified into four: winter (December–February), pre-monsoon (March–May), monsoon (June–August), and post-monsoon (September–November) (Santra, 2025). This study examined the influence of meteorological parameters on particulate matter concentrations across months and seasons throughout 2024 to better understand dispersion and accumulation behaviour. Principle parameters such as ambient temperature, relative humidity, atmospheric pressure, and wind speed were measured on-site at each sampling locations (S1-S70) using a portable Environment Meter (SP-9202) (Figure 3), concurrently with PM sampling. Instrument accuracies were approximately ±0.5 °C, ±3% RH, ±0.1 atm, and ±0.3 m s^{-1}, respectively. Multiple readings were averaged to obtain site-specific daily mean values, which were subsequently integrated with PM concentrations for spatial analysis (Tella & Balogun, 2021; Bilal *et al*., 2019; Safarov *et al*., 2024; Santra, 2025).



FIG 3. Environment meter

2.4 PM Sampling

Size-segregated fractions including $PM_{2.5}$, PM_{1}, $PM_{0.5}$, $PM_{0.25}$, and $<PM_{0.25}$ µm were collected using the cascade impactor (Figure 4) at a constant flow rate of 9.3 L min^{-1}, following gravimetric protocols specified in IS 5182 (Part 4): 1999, (Chauhan *et al*., 2024; Sneha *et al*., 2024). Particulate Matter sampling was conducted across 70 sites. The sampler was mounted at a standardized height of 1.5–2 m at human nose level and was carried by the tester in a school bag, by imparting it in a pipe projection. PTFE filters were conditioned for 24 hours at 27 °C and weighed pre- and post-sampling using an electronic microbalance (Shimadzu AUW220D). The heavy metals in each stage A-D and after-filter were analysed, were detected through ICP-MS test along with their concentrations at each location. In accordance with Indian standards and USEPA guidelines quality assurance and control procedures included filter conditioning, field blanks, flow verification, and microbalance precision checks, (USEPA, 2011; CPCB, 2022).

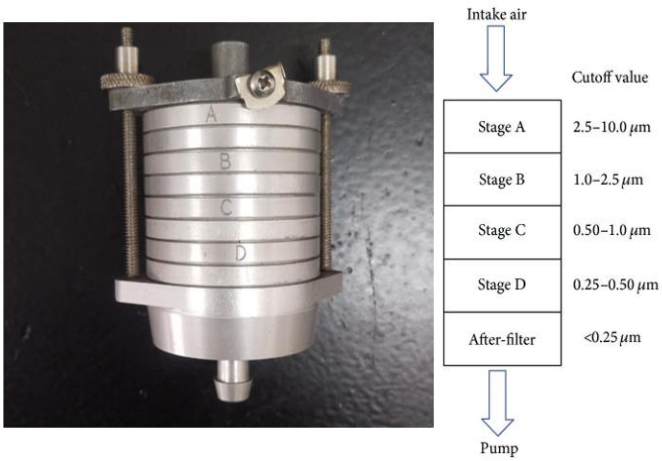


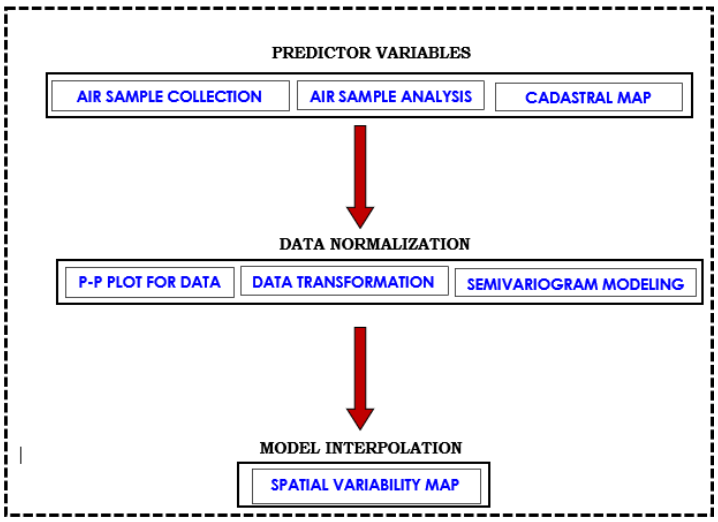
FIG 4. Cascade Impactor

2.5 Diverse Spatial Analysis and Interpolation of PM Dispersion Using GIS

(Figure 5) Outlines the analytical workflow: GIS data preparation → descriptive statistics and normality assessment → IDW interpolation based on proximity weighting → spatial mapping of particulate matter across settlement types.

Spatial distribution of Size-segregated fractions including $PM_{2.5}$, PM_{1}, $PM_{0.5}$, $PM_{0.25}$, and $<PM_{0.25}$ µm throughout the study area were assessed using a widely applied air quality modelling using Inverse Distance Weighting (IDW) interpolation method (Shukla *et al*., 2019).This method assumes a meaningful clout on nearby observations than distant values, making it particularly suitable for

particulate variability in urban environments that are source specific (Choi & Chong, 2022).Descriptive statistical analysis and normality checks were performed, before interpolation, with Box–Cox transformation. Due to dense monitoring network and local-scale heterogeneity, IDW was adopted without imposing spatial stationarity assumptions (Ismain *et al*., 2023). Thus the interpolated surfaces generated 2D maps to examine the spatial pattern of particulate matter across different settlement categories (Safarov *et al*., 2024). Correlation analysis revealed that particulate matter concentrations in Coimbatore are strongly governed by winter meteorological conditions, when



compared to all other seasons and follows a consistent pattern reported in other Indian and global urban environments (Li et al., 2021).

FIG 5. Flow chart using modelling predictions

3.3 Human Health Risk Assessment

Severity of this particulate matter can be analysed using health risk assessment studies and thus this study identifies the health index caused due to $PM_{2.5}$ in the sampling locations for the highest concentrations recorded in January. According to the USEPA and WHO, particulate matter ($PM_{2.5}$) contributes to adverse effects on respiratory, cardiovascular, and neurological health. Thus the non-carcinogenic risk using the Hazard Quotient (HQ) and Hazard Index (HI) methods from $PM_{2.5}$ is evaluated following the methodology established by the United States Environmental Protection Agency (US EPA).

3.3.1 Estimation of Human Exposure Concentration

Exposure dose refers to the Concentration of an external substance or agent that an individual encounters over a defined period. In this study, exposure dosage was estimated for adults aged 20-45

years, representing early adulthood through middle age. The exposure concentration (EC) was calculated at a height of 1.5 m, corresponding to the average breathing zone of a human.

The EC, expressed in µg/m³, was determined using the formula recommended by the US EPA (2004) (Table 2); Risk Assessment Guidance for Superfund (2009) and (Jena *et al*., 2019; Abidin *et al*., 2024).

$$EC = (C*ET*EF*ED)/AT \quad \text{----- Equation (A.1)}$$

TABLE 2. Exposure Variables and Assumed Values for Exposure Concentration (EC) Calculation

Definition (Unit)	**Assumption / Values**	**References**
C – Concentration of element in ambient air (µg/m³)	Measured in $PM_{2.5}$ samples	---
ET – Exposure time (h/day)	8 h/day	---
EF – Exposure frequency (daysyear)	245 days/year	2024 Jan to 2024 Dec
ED – Exposure duration (years)	30 years (adults)	United States Environmental Protection Agency, 2004b; Jena *et al*., 2019
AT – Averaging time (days)	AT = 365 × ED (non-carcinogenic)	United States Environmental Protection Agency, 2004b; Abidin *et al*., 2024

3.3.2 Health Risk Assessment Using Hazard Quotient and Hazard Index

The non-carcinogenic risk associated with $PM_{2.5}$ exposure and other heavy metals associated with this study was evaluated using the Hazard Quotient (HQ) and Hazard Index (HI) methods proposed by the US EPA (Table 3) and (Table 4).

$$HQ = EC/ (RfCi *1000) \quad \text{----- Equation (A.2)}$$

The overall Hazard Index (HI) represents the cumulative risk from multiple pollutants, and calculated as:

$$HI = \Sigma(HQi) \text{ where } i = 1 \text{ to } n \quad \text{----- Equation (A.3)}$$

TABLE 3. Definition and values of parameters used for non-carcinogenic health risk assessment.

Definition (Unit)	Assumption / Values	References
HQ – Hazard Quotient	Ratio to evaluate non-carcinogenic risk from inhalation exposure.	United States Environmental Protection Agency, 1989; USEPA, 2018
EC – Exposure concentration (µg/m³)	Estimated concentration inhaled during exposure period.	USEPA
RfCi – Inhalation reference concentration (mg/m³)	Approximation of daily inhalation exposure level likely to be without significant adverse health effects during a lifetime.	USEPA, 1989
HI – Hazard Index	Sum of hazard quotients of all trace elements to evaluate overall non-carcinogenic risk.	USEPA

TABLE 4. Reference concentration (RfC) values of heavy metals

Metal	RfC (mg/m³)	Reference
Pb (Lead)	2.00×10^{-4}	Cesaro *et al*., 2019; Izhar *et al*., 2016; Morakinyo *et al*., 2021; Sakunkoo *et al*., 2022; USEPA, 2023; Zheng *et al*., 2015; Abidin *et al*., 2024
Cd (Cadmium)	1.00×10^{-5}	Same references
As (Arsenic)	1.50×10^{-5}	Same references
Mn (Manganese)	5.00×10^{-5}	Same references
Cu (Copper)	1.40×10^{-1}	Same references
Zn (Zinc)	1.05	Same references

Fe (Iron)	0.7	Same references

An HI > 1 indicates potential non-carcinogenic health risks, whereas an HI < 1 suggests that adverse health effects are unlikely. Life Expectancy Impact Estimation :

Assuming a linear relationship between HI and life expectancy reduction:

- HI = 2 corresponds to an approximate decrease of 5 years.
- HI = 1 corresponds to an approximate reduction of 2.5 years.

3. RESULT AND DISCUSSION

3.1 Meteorological Parameters and influence on particulate matter

3.1.1 Temperature

Summer (March–May) records the highest temperatures (32–33 °C), and influences PM behaviour through its effects on vertical mixing and atmospheric stability. An increase in temperature can enhance vertical mixing and promote the formation of secondary PM (sulphates, nitrates, secondary organic aerosols, and ammonium salts) (Aldegunde *et al*., 2022; Bose & Roy Chowdhury, 2023). Winter (December–February) is characterized by moderate temperatures (27–28 °C), indicating that lower winter temperatures are associated with reduced boundary-layer height and limited vertical mixing. These conditions favour the accumulation of particulate matter at the near-surface increasing their ground level PM concentrations at all the sampling locations (Ziernicka-Wojtaszek *et al*., 2024).

3.1.2 Relative Humidity

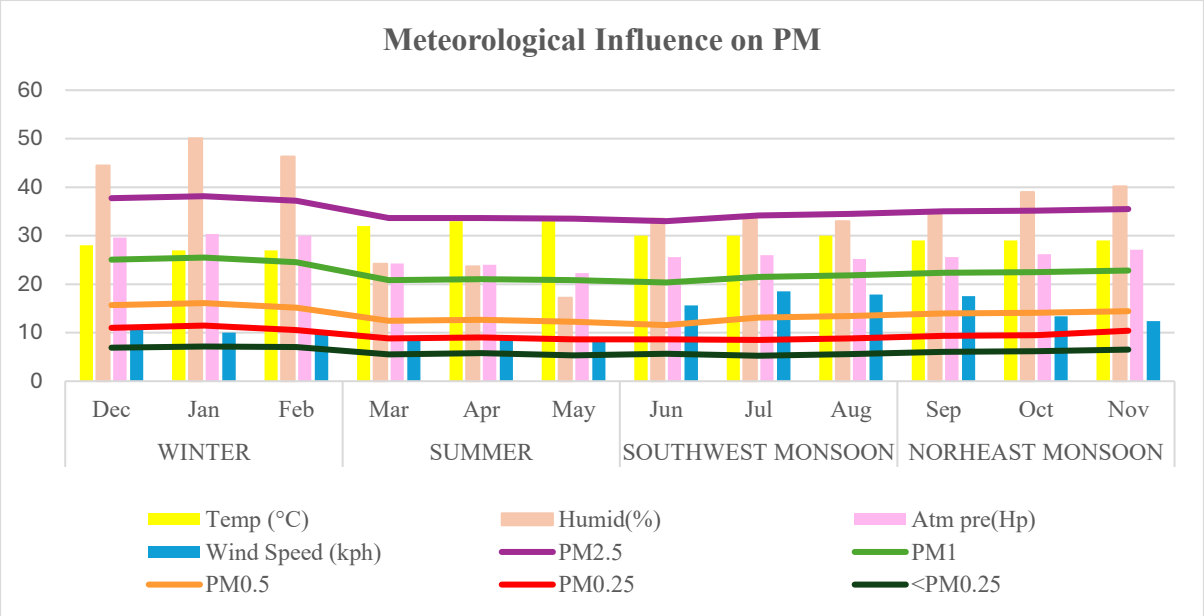
During Winter relatively higher humidity ranges from (44–50%). Humidity affects PM concentration through particle hygroscopicity and secondary aerosol formation. High humidity promotes hygroscopic growth, increasing particle size and potentially facilitating secondary PM formation (Sirithian & Thanatrakolsri, 2022; Zhang *et al*., 2022). These elevated values, common in rural and semi-urban areas, are linked to nearby vegetation, mountains, and water bodies that enhance evapotranspiration (Cheng *et al*., 2015) Conversely, reduced humidity in summer (17–24%) can lead to resuspension of PM from surfaces and are of surfaces and with dense residential areas where reduced vegetation limits evapotranspiration (Ziernicka-Wojtaszek *et al*., 2024).

3.1.3 Atmospheric Pressure

Higher atmospheric pressure (29.6–30.35 Hg during winter (December–February) can lead to temperature inversions, suppressing vertical air movement and increasing ground-level PM concentrations (Xu *et al*., 2014; Han *et al*., 2015). Unstable atmospheric conditions due to low pressure during summer (March–May) ranged from (22.3–24.25 Hg) enhance PM dispersion, and its effects may be modified by local structures such as high-rise buildings in urban areas

3.1.4 Wind Speed

Underscoring wind speed, Southwest Monsoon (June–September) ranged the highest from (15.61–18.5 kph) act as the dominant meteorological parameter governing particulate dispersion. Strong winds enhance horizontal dispersion, transporting PM over long distances and diluting local concentrations. However, low wind speeds (8.85–9.17 kph) under calm weather conditions during Summer (March–May) reduce atmospheric mixing, allowing pollutants to accumulate near the source and increasing ground-level PM concentrations (Ziernicka-Wojtaszek *et al*., 2024). They can also resuspend particles from surfaces, contributing to elevated short-term concentrations (Danek *et al*., 2022). From the current study, highest wind speeds were generally observed in rural areas, while the lowest were recorded in urban zones. This is likely due to building-induced wind obstruction and reduced



ventilation corridors.

FIG 6. Graphical representation of the relationship between seasonal meteorology and PM

Similar meteorological influence is seen across all sizes of PM ($PM_{2.5}$, PM_{1}, $PM_{0.5}$, $PM_{0.25}$, and $<PM_{0.25}$) and varies across seasons (Figure 6). Since, winter concentrations are higher they are taken

for spatial analysis and concentration distribution predictions across the study area. Winter (December–February) is characterized by moderate temperatures (27–28 °C), relatively higher humidity (44–50%), higher atmospheric pressure (29.6–30.35 Hg and weak ventilation particularly enhance pollutant stagnation in dense dump zone, urban and traffic-dominated zones, comparatively low wind speeds (9.98–10.94 kph), indicating stable atmospheric conditions with limited dispersion potential and higher health risks among various sensitive groups (Aron *et al*., 2024).

3.2 SPATIAL DISPERSION

As discussed previously winter season poses severe particulate pollution during the study period in Coimbatore. Accordingly, the peak $PM_{2.5}$, PM_{1}, $PM_{0.5}$, $PM_{0.25}$, and $<PM_{0.25}$ pollution in January is taken for spatial predictions (Figure 7) which has worst-case concentrations when compared to December and February. Spatial localization increased systematically with decreasing particle size, highlighting stronger source-proximity effects for ultrafine fractions.

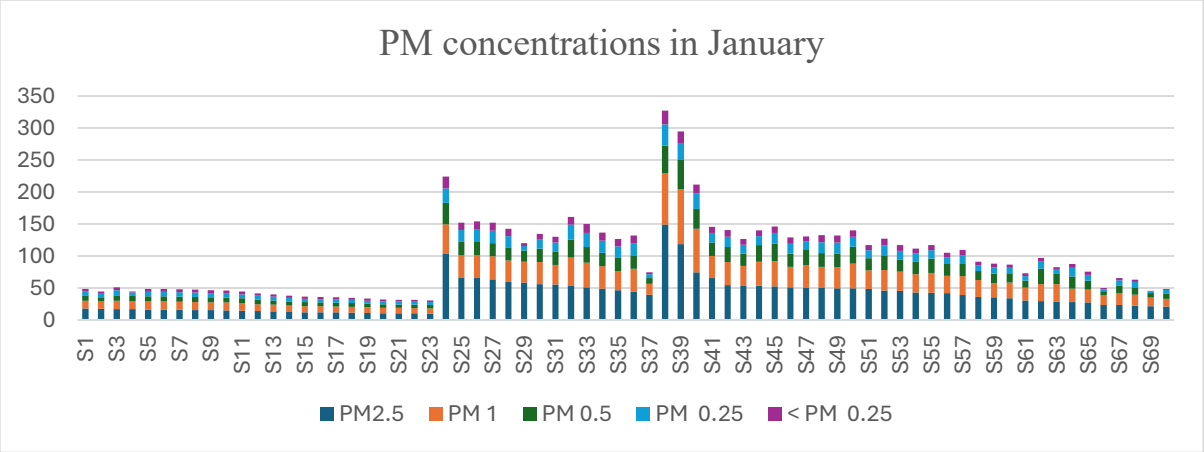


FIG 7. PM Concentrations for the winter peak January

3.2.1 Spatial Distribution of $PM_{2.5}$ – Coarse Particles

Strong meteorological conditions and emission intensity originating from both natural and anthropogenic sources contribute to $PM_{2.5}$ particles in Stage A (2.5–10 µm) (Ravindra *et al*., 2021; Li *et al*., 2021). During winter, $PM_{2.5}$ concentrations across Coimbatore exhibited pronounced spatial heterogeneity, ranging from 10.1 to 149.1 µg/m³, with a seasonal mean of 44.2 ± 28.7 µg/m³. Higher concentrations of $PM_{2.5}$ were recorded in S38–S58 within central and north-central urban–industrial zones, particularly near the Vellalore dump yard and major transport corridors (NH 181, NH 544, SH 162) (Lee *et al*., 2006). Major sources $PM_{2.5}$ are tons of open organic and inorganic waste deposition of more than 10 years (Soumiya *et al*., 2018). windblown dust, home-related emissions,

factories and industries emissions, power plant generation, landfill fires, waste handling, transportation emissions, chemical and meteorological influence on dump in open environment (Lei & Ma, 2023; Jain *et al*., 2021; AQI 2026) are the main source of $PM_{2.5}$ in all the sampling locations.

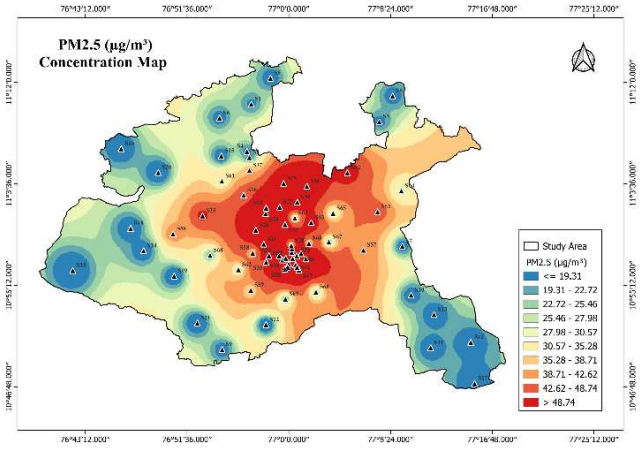


FIG 8. Spatial Dispersion of $PM_{2.5}$

(Figure 8) reveals a distinct urban–rural gradient, with high $PM_{2.5}$ levels (>80 µg/m³) along dump yard, central transport and industrial belts, moderate concentrations (40-70 µg/m³) in semi-urban transition zones, and the lowest levels (10-20 µg/m³) in peripheral rural areas characterized by open terrain and vegetation cover. This spatial pattern underscores the combined effects of Source density, urban morphology, population distribution across various locations, various activities, emission sources and suppressed winter boundary-layer height restrict vertical dispersion and promote pollutant accumulation (Murthy *et al*., 2020; Li *et al*., 2021; Hsu *et al*., 2017).

3.2.2 Spatial Distribution of PM_1 – Fine Particles

PM_1 in Stage B (1.0–2.5 µm) is formed predominantly through chemical reactions in the atmosphere, especially via the conversion of volatile organic compounds (VOCs) into secondary organic aerosols (SOAs). Combustion processes, both natural and anthropogenic, also contribute to PM1 formation. During winter, PM_1 concentrations ranged from 8.0 to 86.1 µg/m³, with a mean of 30.5 ± 17.6 µg/m³ near S38–S58 due to residing dump and combined influence of NH 181, NH 948 (Lee *et al*., 2006)., multi-speciality hospitals, and educational institutions, which collectively increase secondary pollutant formation at the central urban sector. PM_1 levels are closely linked to ,landfill fires, decomposing waste emission, waste handling equipment (diesel machinery), road dust re-suspension, vehicular emissions (diesel exhaust), industrial emissions (foundries and textile units), brick kilns, construction activities, open burning of waste and residential combustion sources which intensify under winter stagnation (Li *et al*., 2021; Chakraborty & Gupta, 2024).

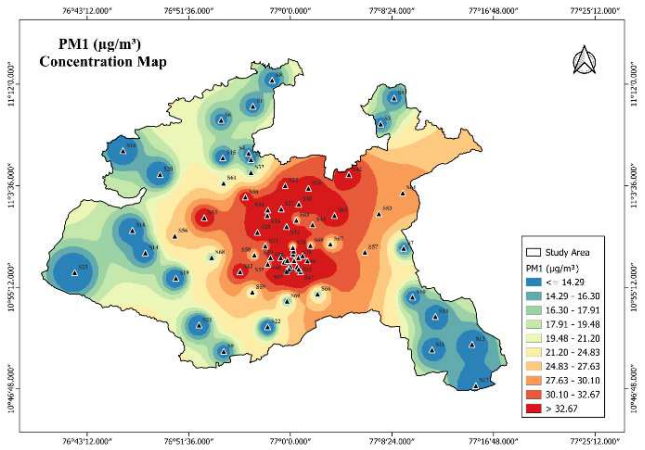


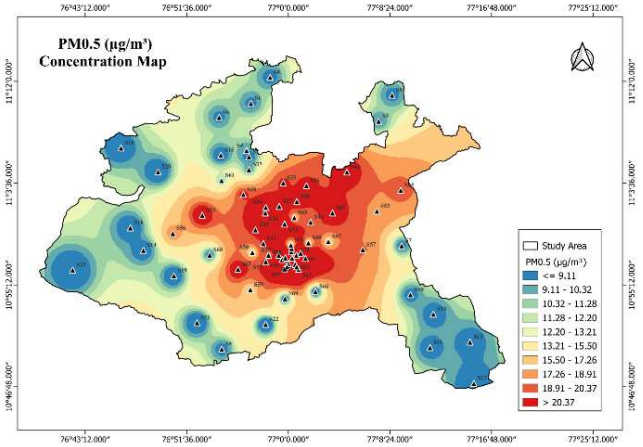
FIG 9. Spatial Dispersion of PM_1

(Figure 9) illustrates that central and north-central industrial corridors has elevated PM_1 concentrations (>33 µg/m³). Semi-urban regions exhibited moderate levels (18–32 µg/m³), while peripheral rural zones showed comparatively lower concentrations due to reduced emission intensity and enhanced ventilation. The persistence of elevated PM_1 in urban hotspots underscores the dominance of fine combustion aerosols and weak atmospheric mixing during winter.

3.2.3 Spatial Distribution of $PM_{0.5}$ - Ultrafine particles (UFP fraction)

As per monitoring these ultrafine particles $PM_{0.5}$ in Stage C (0.50–1.0 µm) originates primarily from atmospheric nucleation reactions (secondary particle formation). $PM_{0.5}$ concentrations ranged from 6.2 to 45.2 µg/m³ during winter, with a mean of 20.5 ± 10.4 µg/m³. Sites S39 and S48–S60 observed peak values , particularly near NH 544 and SH 162. This is due to high traffic density, industrial activity, and secondary aerosol formation substantially contributed to ultrafine particle loading, traffic-related gaseous precursor emissions, industrial combustion emissions, metallic and carbonaceous ash from combustion, diesel engine exhaust (nucleation mode particles), indoor biological aerosols (bacteria and viruses), fine pet/animal dander. (Choi & Chong, 2022; Li *et al*., 2022, Nkansah F.K. *et al*.2025).

(Figure 10) illustrates that the $PM_{0.5}$ concentrations (>20 µg/m³) tightly confined at central and north-central Coimbatore, while semi-urban zones recorded intermediate levels (10–20 µg/m³). Due to

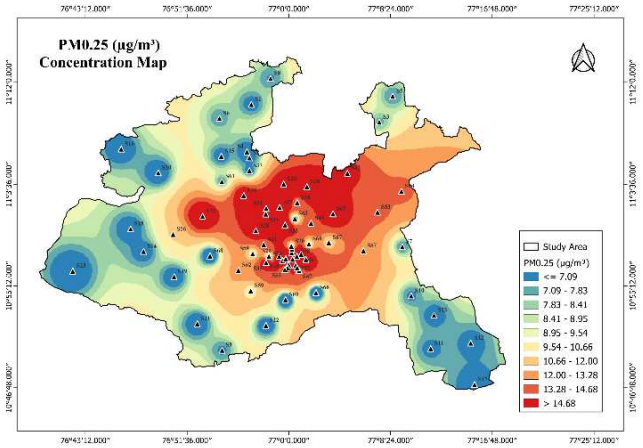


reduced anthropogenic influence rural fringes consistently exhibited low concentrations (<9 µg/m³), reflecting reduced and enhanced dispersion in open landscapes. stronger spatial localization was observed in $PM_{0.5}$ compared with $PM_{2.5}$, underscoring its heightened sensitivity to nearby combustion sources and wintertime atmospheric stability.

FIG 10. Spatial Dispersion of $PM_{0.5}$

3.2.4 Spatial Distribution of $PM_{0.25}$ - Very ultrafine particles

$PM_{0.25}$ in Stage D (0.25–0.50 µm) originates mainly from high-temperature industrial processes (metal processing, smelting, welding), municipal waste incineration and coke calcination, high-temperature cooking (frying, grilling, broiling), atmospheric nucleation from So_2, No_x, and VOC's, diesel engine exhaust and high-temperature combustion emissions. During winter, $PM_{0.25}$ concentrations ranged from 3.0 to 32.8 µg/m³, with a mean of 14.8 ± 8.0 µg/m³. The highest values were recorded at (S38 – S53), located in traffic-intensive and industrial regions where ultrafine particle emissions from



combustion and secondary processes dominate.

FIG 11. Spatial Dispersion of $PM_{0.25}$

(Figure 11) Central and mid-eastern Coimbatore illustrates $PM_{0.25}$ hotspots (>14.5 µg/m³) , while semi-urban belts exhibited moderate concentrations and rural peripheries showed the lowest levels (<7 µg/m³). The steep urban–rural gradient highlights the limited atmospheric transport of ultrafine particles and their strong dependence on local emission density under stable winter conditions.

3.2.5 Spatial Distribution of <$PM_{0.25}$ - Nanoparticles

The ultrafine fraction <$PM_{0.25}$, comprising particles smaller than 0.25 µm collected on the after-filter, includes nanoparticles generated from the breakdown of $PM_{0.25}$ and secondary chemical processes, resuspended road dust (unpaved roads, traffic movement, tire and brake wear), construction and demolition activities, industrial emissions (foundries, engineering units, textile mills), brick kilns in semi-urban areas, wind-blown soil dust from dry surfaces and open lands, agricultural activities in surrounding rural belts (tilling and ploughing), biomass and wood burning (including open waste burning). Concentrations ranged from 1.3 to 21.8 µg/m³, with a mean of 7.5 ± 4.4 µg/m³. The highest values were observed at S38 - S53, situated within urban–industrial corridors (Nkansah *et al*.,2025)Li *et al*., 2021; Choi & Chong, 2022).

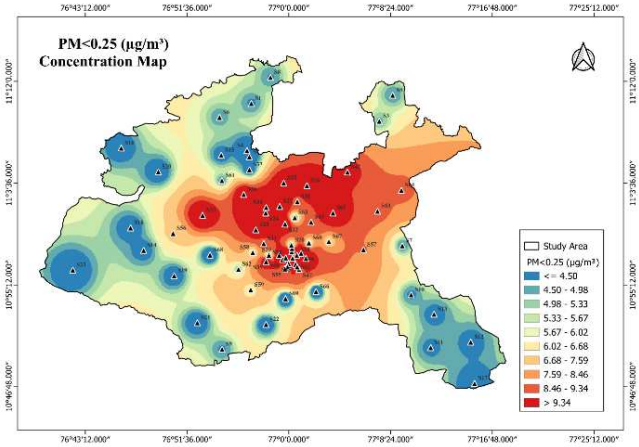


FIG 12. Spatial Dispersion of <$PM_{0.25}$

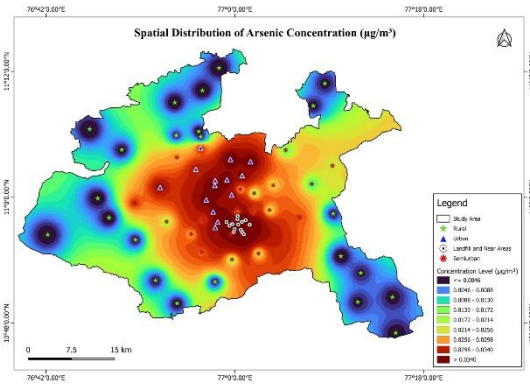
(Figure 12) illustrates strong spatial clustering of nano particles in central and eastern Coimbatore (>9 µg/m³), with concentrations declining sharply toward semi-urban and rural areas. Due to their high reactivity and short atmospheric lifetimes, ultrafine particles exhibit pronounced localization near emission sources, with winter accumulation strongly influenced by a reduced boundary-layer height and weak ventilation.

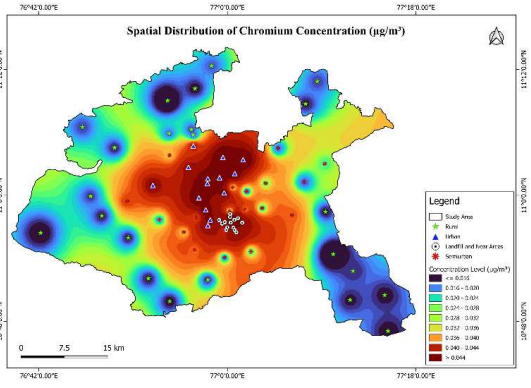
3.3 Spatial Distribution and Source Characteristics of Heavy Metals

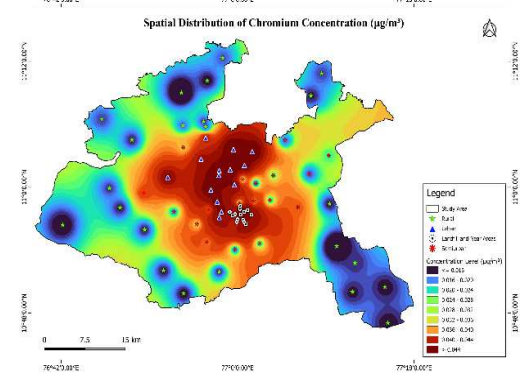
TABLE 5. Average values of HMs in each zone during winter

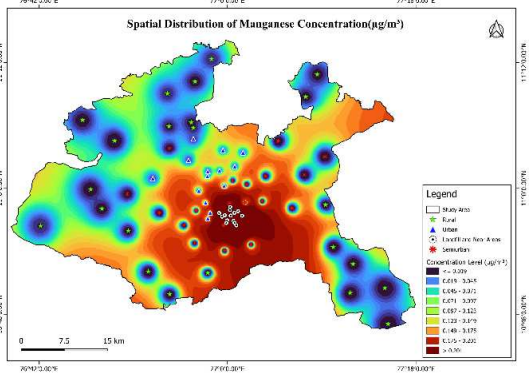
METALS	CL (LANDFILL)	CU (URBAN)	CS (SEMI-URBAN)	CR (RURAL)
As	0.0456	0.0394	0.0223	0.0020
Cd	0.0274	0.0222	0.0111	0.0040
Cr	0.0467	0.0521	0.0267	0.0146
Ni	0.0428	0.0697	0.0395	0.0066
Pb	0.2250	0.2250	0.2250	0.0062
Mn	0.3773	0.0258	0.0097	0.0121
Cu	0.7550	0.2175	0.1270	0.0259
Zn	1.3178	1.7200	1.0594	0.0862
Fe	10.9152	7.9033	5.0510	2.0367

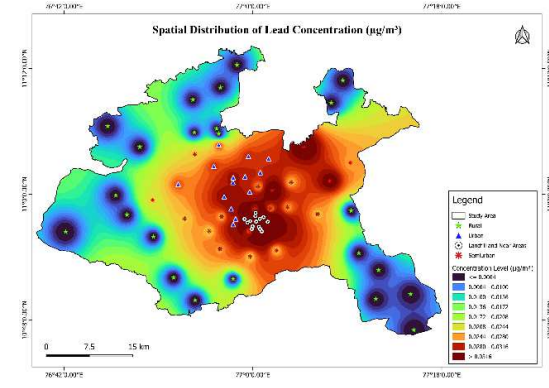
(Table 5) The spatial distribution of heavy metals (HMs) in $PM_{2.5}$ over the study area (Figure 13-21). is classified into four different zones: landfill-influenced, urban, semi-urban, and rural. Higher mean concentrations of heavy metals were observed during the winter season across all zones. This is mainly due to unfavourable meteorological conditions, including low wind speed, atmospheric stagnation, high humidity, and temperature inversion, which reduce turbulence. These conditions enhance pollutant accumulation and limit dispersion. A consistent pattern is observed in all maps of heavy metals suggesting a common controlling factor influencing the spatial variability, higher concentration predominantly representing red and dark orange colour occurs in the central regions were transitioning to moderate levels are represented by orange to yellow in the surrounding area and such the lower concentration towards the peripheral zones are represented by green to blue colour.

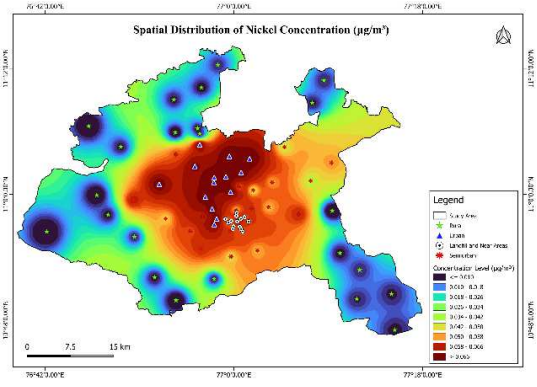

Spatial Distribution of Arsenic Concentration (µg/m³)
Legend
Study Area
Rural
Urban
Landfill and Near Areas
Semiurban
Concentration Level (µg/m³)
0 7.5 15 km

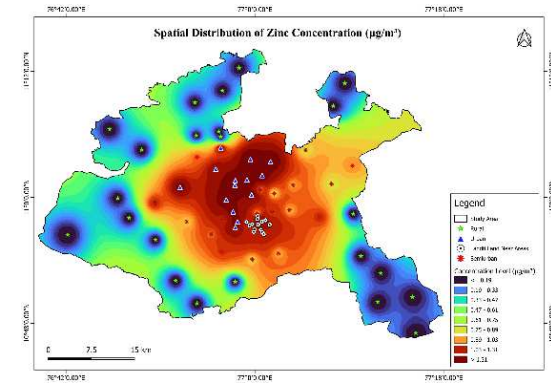

Spatial Distribution of Chromium Concentration (µg/m³)
Legend
Study Area
Rural
Urban
Landfill and Near Areas
Semiurban
Concentration Level (µg/m³)
0 7.5 15 km

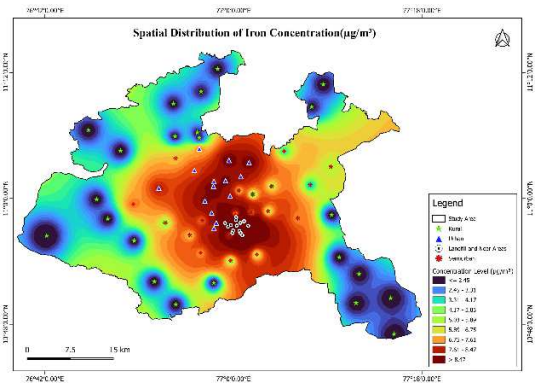

Spatial Distribution of Chromium Concentration (µg/m³)
Legend
Study Area
Rural
Urban
Landfill and Near Areas
Semiurban
0 7.5 15 km


Spatial Distribution of Manganese Concentration(µg/m³)
Legend
Study Area
Rural
Urban
Landfill and Near Areas
Semiurban
0 7.5 15 km


Spatial Distribution of Lead Concentration (µg/m³)
Legend
Study Area
Rural
Urban
Landfill and Near Areas
Semiurban
0 7.5 15 km


Spatial Distribution of Nickel Concentration (µg/m³)
Legend
Study Area
Rural
Urban
Landfill and Near Areas
Semiurban
0 7.5 15 km


Spatial Distribution of Zinc Concentration (µg/m³)
Legend
0 7.5 15 km


Spatial Distribution of Iron Concentration(µg/m³)
Legend
Study Area
Rural
Urban
Landfill and Near Areas
Semiurban
0 7.5 15 km

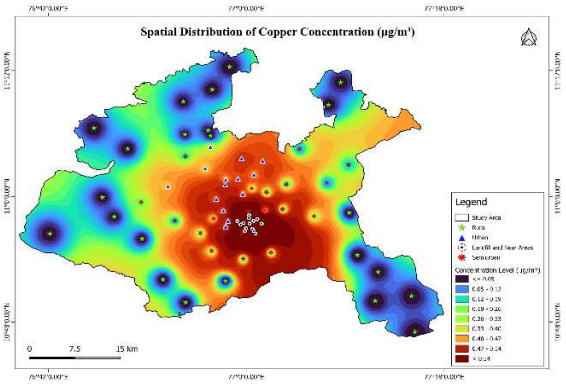


FIG 13-21. Spatial distribution of HMs over the study area

The dominance of Fe and Zn across all zones confirms crustal resuspension and road dust contributions, consistent with CPCB (2023). The landfill-influenced zone is identified as a high-impact zone representing (dark red/red zones) of HMs. Areas such as Chettipalayam and Kovai Mahalingapuram (S38–S52), have recorded significantly elevated Fe, Cd, Pb, Zn, Cu concentrations. The order of heavy metal concentrations in this zone following the order Fe > Cu > Zn > Mn > Pb > Cr > As > Cd > Ni, indicates that increased emission levels are primarily due to continuous emissions from landfill activities and associated anthropogenic sources (Table 6). Higher concentrations of metals identified in these regions due to continuous emissions from waste decomposition, open burning, leachate drying, and mechanical disturbance of waste materials. The landfill zone shows distinct enrichment of Mn, Cu, Fe, indicating solid waste combustion and decomposition p rocesses, consistent with Njoku *et al*. (2019) and Palmiotto *et al*. (2014).

Urban regions, including Gandhipuram, Peelamedu, and Ramanathapuram (S24–S37), exhibited similarly high HM concentrations (red/orange zones), driven by intense anthropogenic activities. The observed concentration trend Fe > Zn > Cu > Pb > Cr > Ni > Mn > As > Cd reflects combined contributions and indicates high emission intensity in these areas. The dominant sources (Table 6) were identified as vehicular emissions contributing to Pb, Zn, and Cu, along with brake and tyre wear contributing significantly to Cu and Zn, while fuel combustion processes were responsible for Ni and Cr, as detailed in Table 4. This zone represents the core pollution plume of the study area. Elevated Pb, Cu, Zn in urban areas clearly indicate traffic-related emissions, supported by Karagulian *et al*. (2015) and Nkansah *et al*. (2025).

Semi-urban areas (S38–S70), such as Vellalore, Kuniyamuthur, Sulur, and Neelambur, showed moderate HM concentrations (yellow–orange zones) with a slightly altered trend Fe > Zn > Cu > Pb > Ni > Cr > As > Cd > Mn, indicating mixed influences from urban expansion, small-scale industries,

agricultural practices, and construction activities. Noticeable hotspots especially for Cr, Ni, Mn, Fe. These transitional zones exhibit a combination of emission sources (Table 6), including road dust, fuel combustion, and informal recycling, cement, metal processing as presented in Table 4. This zone Indicates industrial influence with localized dispersion patterns. Semi-urban regions exhibit intermediate characteristics, confirming mixed source contributions, as reported by Bilal *et al*. (2019).

The rural regions (S1–S23) ,including Anaikatti and Navakkarai, recorded the lowest HM concentrations (blue–green zones) with the order of metals as Fe > Zn > Cu > Cr > Mn > Ni > Pb > As > Cd. The reduce background/baseline concentrations of all the metals in these areas are linked to minimal direct anthropogenic influence. The presence of vegetation cover, agricultural land, and green spaces, open lands, reduced population and construction activities aid in pollutant dispersion and deposition. Low variability in rural As and Cd is due to localized contamination (S23), which aligns with findings of Khan *et al*. (2020) and Roy *et al*. (2019) on spatial heterogeneity.

TABLE 6. Identified sources of PM Fractions and Heavy Metals

ZONE	SAMPLING LOCATIONS	PM FRACTIONS + HEAVY METALS	MAJOR SOURCES	TYPICAL ACTIVITIES / PROCESSES
LANDFILL AREAS	Dump Yard (S38)	$PM_{2.5}$, PM_{1}, $PM_{0.5}$, $PM_{0.25}$, <PM0.25 + Pb, Cd, Cu, Zn, Fe	Waste screening, segregation, e-waste handling (Njoku *et al*., 2019; Palmiotto *et al*., 2014; Meena *et al*., 2023)	Mechanical sorting, organic waste processing, metal scrap handling
		$PM_{2.5}$ + Pb, Cd	Battery waste (Khan *et al*., 2020; CPCB, 2023)	Dry/rechargeable batteries
		PM_{1} + Fe, Cu, Zn	Metallic waste (Soumiya *et al*., 2018; Meena *et al*., 2023)	Scrap, construction debris
		$PM_{2.5}$, PM_{1} +	Waste transport	Truck movement,

		Multiple metals	(Njoku *et al*., 2019)	dust generation
		$PM_{0.25}$, <PM0.25 + Pb, Cd, Cu	Informal recycling (Khan *et al*., 2020; Sah, 2022)	Burning wires, dismantling electronics
URBAN AREAS	Gandhipuram (S24), Town Hall (S28), Peelamedu (S30), others (S25–S27, S29–S37)	$PM_{2.5}$, PM_{1}, $PM_{0.5}$, $PM_{0.25}$, <PM0.25 + Pb, Cr, Cd, Ni, Cu, Zn, Mn, Fe	Vehicular emissions, electroplating, industries, generators (Karagulian *et al*., 2015; CPCB, 2022; Nkansah *et al*., 2025)	Traffic congestion, automobile workshops, AC servicing, welding, fabrication, construction, e-waste handling
		$PM_{2.5}$ (dominant) + Pb, Zn	Brake and tyre wear (Karagulian *et al*., 2015; Jain *et al*., 2021)	High traffic roads, transport hubs
		PM_{1}, $PM_{0.5}$ + Cr, Ni, Fe, Mn	Industrial processes (Sharma *et al*., 2023; Gupta *et al*., 2020)	Foundries, furnaces, metal processing
		$PM_{0.25}$, <PM0.25 + Cd, Pb, Cu	E-waste recycling (Khan *et al*., 2020; Sah, 2022)	Electronic dismantling units
PERI-URBAN AREAS	Dump Yard (S38), Chettipalayam (S39), Kovai Mahalingapuram (S40), others (S41–S70)	$PM_{2.5}$, PM_{1}, $PM_{0.5}$, $PM_{0.25}$, <PM0.25 + Pb, Zn, Cu, Fe	Mixed traffic and road dust (Karagulian *et al*., 2015; Bilal *et al*., 2019)	Highways, connecting roads
		$PM_{2.5}$ + Cr, Ni, Mn, Fe	Small-scale industries (Gupta *et al*., 2020; Kumari	Fabrication, welding, small foundries

			et al., 2021)	
		$PM_{0.5}$, $PM_{0.25}$ + Cd, Pb, Cu	Informal recycling (Khan *et al*., 2020; Sah, 2022)	Scrap yards, roadside e-waste
		$PM_{2.5}$ + As, Cd, Cu, Zn	Agricultural + urban mix (Jena *et al*., 2019; Kumari *et al*., 2021)	Fertilizers, pesticide use
		PM_{1} + Fe, Mn, Zn	Construction and land-use change (Bilal *et al*., 2019; CPCB, 2022)	Soil excavation, development
		$PM_{2.5}$ + Pb, Zn, Cu	Waste burning (Meena *et al*., 2023; WHO, 2021)	Open dumping and burning
		PM_{1}, $PM_{0.5}$ + Ni, Cr, Fe	Fuel combustion (Karagulian *et al*., 2015; Jain *et al*., 2021)	Diesel generators, brick kilns
RURAL AREAS	Jothipuram (S1), Anaikatti (S16), Navakkarai (S21), others (S2–S23)	$PM_{2.5}$, PM_{1}, $PM_{0.5}$, $PM_{0.25}$, <PM0.25 + Fe, Mn, Zn	Soil dust (Bilal *et al*., 2019; CPCB, 2022)	Agricultural tilling, wind erosion
		$PM_{2.5}$ + As, Cd, Cu	Agricultural inputs (Jena *et al*., 2019; Kumari *et al*., 2021)	Fertilizers, pesticides
		$PM_{2.5}$ + Pb, Zn	Biomass burning (WHO, 2021; Manisalidis *et al*., 2020)	Crop residue burning
		PM_{1}, $PM_{0.5}$ + Ni, Cr, Fe	Natural sources (Sharma *et al*.,	Rock weathering

			2023; Gupta *et al*., 2020)	
		PM_1 + Fe, Mn	Road dust (Bilal *et al*., 2019)	Rural transport
		$PM_{0.5}$ + Cu, Zn	Equipment wear (Karagulian *et al*., 2015)	Agricultural machinery

3.3.2 Health Risk Assessment and Spatial Correlation

HI distribution and $PM_{2.5}$ concentration patterns has strong spatial correspondence indicating that fine particulate matter acts as an effective carrier for heavy metals and the non-carcinogenic health risk assessment enhances inhalation exposure health risks among human being and evaluates the reduced life span of human population at each zone in Table 5. The average HI values followed the order: Landfill (4.28) > Urban (2.96) > Peri-urban (1.73) > Rural (0.40). The cumulative Hazard Index (HI) across different zones are presented in (Figure 22).

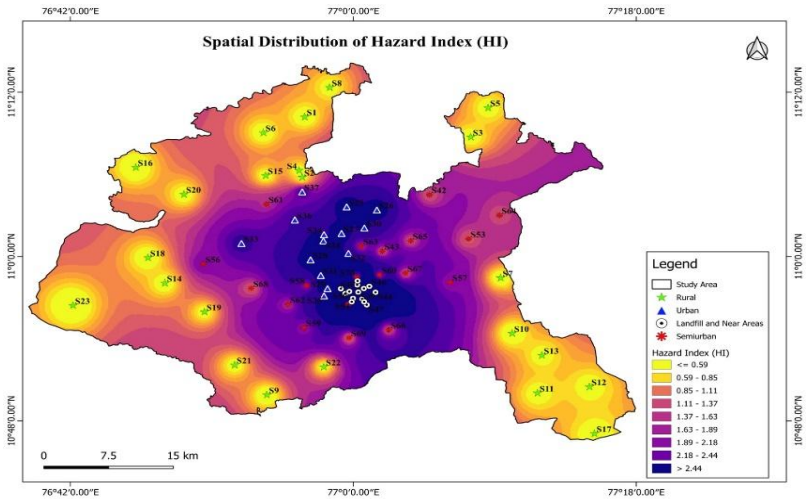


FIG 22. Hazard index over different sample locations

The highest non-carcinogenic risk was exhibited in landfill-influenced zones (S38–S54) particularly visible as dark blue and blue hotspots. With an average HI value of 4.28, exceeding the safe threshold (HI > 1). The spatial clustering of higher $PM_{2.5}$-bound metal concentrations arising from which collectively intensify exposure in surrounding settlements contribute to higher health risks. Open dumping, waste burning, leachate-related emissions, and dust resuspension are the major contributors for the health risk at these zones. The landfill-influenced zone records the highest impact, with an

average life span reduction of approximately 9 years 4 months, highlighting severe exposure conditions.

The urban core region (S24–S37) represented by dark blue to violet shades predominantly has an average HI value of 2.96 (Table 7), also exceeding the permissible in the central portion of the map. These urban clusters show a consistent spatial pattern of controlled HI levels, with high $PM_{2.5}$-bound emissions and comparatively reduced non-carcinogenic than landfill areas with higher metal concentrations, likely due to the relatively balanced contribution of metals with lower toxicity weights and compositions. High population density, vehicular emissions, and industrial acetozones are the major contributors. The urban zone exhibits significant health risk, with an average life span reduction of approximately 6 years 10 months due to dense population and emission sources.

The peri-urban and industrial regions (S55–S70) surrounding the central urban core recorded an average HI value of 1.73 (Table 7), represented by purple to pink colour gradients exhibit moderate HI values with moderate metal concentrations. These zones act as transitional areas where the HI increases outward from the urban centre and has moderate health risks than urban areas. Site-specific emission sources are represented as yellow patches which are the localized hotspots of this zone. They have industrial activities and mixed land-use patterns and expanding anthropogenic activities lower than urban and landfill regions and remain vulnerable due to ongoing urbanisation and industrial spillover effects. The peri-urban zone shows moderate impact, with an average life span reduction of approximately 4 years 5 months, reflecting transitional exposure levels between rural and urban areas.

The rural regions (S1–S23) located far away from the city centre showed the lowest average HI value of 0.40 (Table 7), represented by orange to yellow colours toward the outer periphery has a clear spatial gradient of decreasing non-carcinogenic risk with minimal non-carcinogenic risk than semi urban. These lower values are due to long-range transport, biomass burning, agricultural dust and localized activities. Despite lower pollutant concentrations, relative contribution of more toxic metals (such as Cd and As) plays a significant role in increasing the overall hazard index. The rural zone shows minimal health impact, with an average life span reduction of approximately 0 years 10 months, indicating relatively low exposure levels.

TABLE 7. Life Expectancy Impact Estimation (years) for different zones

ZONE	HI Range	Sampling Locations/Zones	No. Of Samples	Life Span Reduction (Years)	Interpretation

Safe	≤ 1	S1–S23/Rural	22	0.4 – 1.1	No significant health risk; suitable environmental conditions
Moderate	1 – 2	S42, S43, S53, S55–S70/Semi-urban	21	3.0 – 4.9	Potential risk; continuous monitoring required (common near landfill buffer/peri-urban zones)
Critical	> 2	S24–S37, S38–S41, S44–S52, S54/Urban and Landfill	27	5.8 – 12.4	High health risk; likely impacted by landfill emissions / urban-industrial pollution

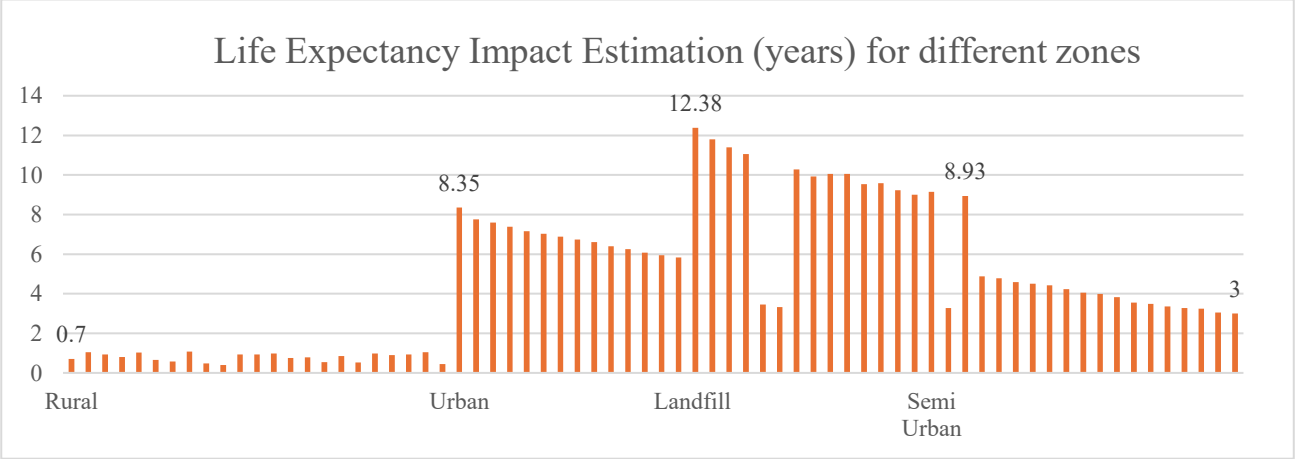


FIG 23. Graphical representation of Life Expectancy Impact Estimation (years) From S1-S70

4. CONCLUSION

The current study on of $PM_{2.5}$, PM_{1}, $PM_{0.5}$, $PM_{0.25}$, and $<PM_{0.25}$ significantly contribute to poor air quality and increased exposure to toxic metals, thereby amplifying public health risks in the Coimbatore city. Focusing on peak seasonal concentrations, the study provides a conservative and forward-looking assessment of air quality under current and future urbanisation pressures during winter conditions. Special discussion on winter conditions plays a critical role in pollutant accumulation due to unfavourable meteorological conditions in the study area. Low mixing heights, atmospheric stability, temperature inversions, suppressing vertical air movement, and reduced dispersion were identified. Integrated field monitoring, spatial distribution of $PM_{2.5}$, PM_{1}, $PM_{0.5}$,

$PM_{0.25}$, and <$PM_{0.25}$, GIS-based spatial modelling, and non-carcinogenic health risk evaluation on $PM_{2.5}$-bound heavy metals exhibited similar spatial trends. The high-resolution spatial mapping demonstrated that ultrafine particles penetrate beyond conventional $PM_{2.5}$ concentration zones, extending into peri-urban and even rural regions, suggesting enhanced transport potential and raising concerns about wider population exposure and the essential and urgent need for more focused studies on ultrafine particles PM_1, $PM_{0.5}$, $PM_{0.25}$, and <$PM_{0.25}$. The alignment between $PM_{2.5}$ hotspots and elevated Hazard Index (HI) values further demonstrates that fine particulate matter plays a key role in controlling the spatial distribution and inhalation risk of heavy metals. The source apportionment and spatial trend followed distinct zone-wise characteristics in the order rural < semi-urban < urban< landfill. This spatial pattern highlights the impact of urbanization and landfill-related emissions. Hazard Index (HI) assessment shows a clear relationship between settlement type and health risk across the study area. The highest pollutant levels were recorded around the Vellalore dump yard, Chettipalayam, Neelambur, and central traffic corridors, identifying as persistent emission hotspots. Landfill-influenced regions(S38-S51) fall within the critical zone (HI > 2), showing significant health risks with life span reduction exceeding 5 years and reaching up to 12 years in some locations. Urban centres (S24–S37) such as Gandhipuram, Saravanampatti, and Town Hall are dominated by vehicular emissions, high population density, clumsy built-up areas which trap pollutants near the road surface, various anthropogenic activities contribute to higher $PM_{2.5}$ and heavy metal concentrations. Semi-urban areas reflect transitional mixed sources. (HI > 2) in the urban zone exhibits significant health risk, with an average life span reduction of approximately 6 years 10 months due to dense population and emission sources. Semi-urban areas (S42, S43, S53, S55–S70) are classified under the moderate zone ($1 < HI \leq 2$), reflecting increasing anthropogenic influence and life span reduction ranging from 3 to 5 years. Rural areas (S1–S23) show crustal dominance with localized anomalies. Rural locations fall within the safe zone ($HI \leq 1$), indicating minimal pollution exposure and negligible life span reduction (below 1.1 years). Beyond direct inhalation risks, elevated fine and ultrafine particulate concentrations along with heavy metals can exacerbate existing respiratory, cardiovascular, and neurological disorders, particularly among sensitive populations. These findings emphasize the urgent need for targeted mitigation strategies, including improved solid waste management, stricter vehicular emission controls, regulation of informal recycling activities, and sustainable peri-urban planning. Continuous monitoring combined with spatially informed policy interventions is essential to reduce exposure levels and ensure long-term public health protection.

Ethical Approval and Consent to Participate

Not Applicable

Competing Interests

The authors declare that they have no competing interests

Authors' contributions:

PALANISWAMY VIVEKANANDAN POOJANANDINE[1*], ARUNACHALAM, GANDHIMATHI[2]

1. **PALANISWAMY VIVEKANANDAN POOJANANDINE (PVP)** Conceptualization, methodology, field investigation, particulate matter sampling and analysis, data curation, statistical analysis, interpretation of results, visualization, manuscript writing – original draft preparation, and revision.
2. **ARUNACHALAM GANDHIMATHI (AG)** Supervision, validation, research guidance, review and editing of the manuscript, interpretation of heavy metal health risk assessment, and overall project administration.All authors read and approved the final manuscript

Availability of data and materials

The datasets used and/or analysed during the current study are available from the corresponding author on reasonable request.

AI Assistance Disclosure

The authors declare that artificial intelligence (AI) tools were not used for the manuscript written.

Funding

No Funding Received (Not Applicable)

Consent for Publication

Not Applicable

REFERENCES

1. Abidin, A.U., Maziya, F.B., Susetyo, S.H., Yoneda, M. and Matsui, Y., 2024. Heavy metal air pollution in an Indonesian landfill site: Characterization, sources, and health risk assessment for informal workers. *Environmental Advances*, *15*, p.100512.
2. Aldegunde JAÁ, Sánchez AF, Saba M, Bolaños EQ, Palenque JÚ. Analysis of PM2.5 and Meteorological Variables Using Enhanced Geospatial Techniques in Developing Countries: A Case Study of Cartagena de Indias City (Colombia). Atmosphere. 2022; 13(4):506. https://doi.org/10.3390/atmos13040506
3. Ali, M.U., Lin, S., Yousaf, B., Abbas, Q., Munir, M.A.M., Rashid, A., Zheng, C., Kuang, X. and Wong, M.H., 2022. Pollution characteristics, mechanism of toxicity and health effects of the ultrafine particles in the indoor environment: Current status and future perspectives. *Critical Reviews in Environmental Science and Technology*, *52*(3), pp.436-473.

4. Aron, J., Baldomero, A.K., Rau, A., Fiecas, M.B., Wendt, C.H. and Berman, J.D., 2024. Individual risk factors of PM2. 5 associated with wintertime mortality in urban patients with COPD. *Chest*, *165*(4), pp.825-835.
5. Bilal, M., Nichol, J.E., Nazeer, M., Shi, Y., Wang, L., Kumar, K.R., Ho, H.C., Mazhar, U., Bleiweiss, M.P., Qiu, Z. and Khedher, K.M., 2019. Characteristics of fine particulate matter (PM2. 5) over urban, suburban, and rural areas of Hong Kong. *Atmosphere*, *10*(9), p.496.
6. Bose, A. and Roy Chowdhury, I., 2023. Investigating the association between air pollutants' concentration and meteorological parameters in a rapidly growing urban center of West Bengal, India: a statistical modeling-based approach. *Modeling Earth Systems and Environment*, *9*(2), pp.2877-2892.
7. Central Pollution Control Board (CPCB). (2022). National air quality status and trends in India. CPCB, New Delhi, India.
8. Central Pollution Control Board (CPCB). (2023). Heavy metals present in air of Indian cities. CPCB, New Delhi, India.
9. Chakraborty, A. and Gupta, T., 2010. Chemical characterization and source apportionment of submicron (PM1) aerosol in Kanpur region, India. *Aerosol and Air Quality Research*, *10*(5), pp.433-445.
10. Chauhan, B.V., Corada, K., Young, C., Smallbone, K.L. and Wyche, K.P., 2024. Review on sampling methods and health impacts of fine (PM2. 5,≤ 2.5 μm) and ultrafine (UFP, PM0. 1,≤ 0.1 μm) particles. *Atmosphere*, *15*(5), p.572.
11. Cheng, Y., He, K.B., Du, Z.Y., Zheng, M., Duan, F.K. and Ma, Y.L., 2015. Humidity plays an important role in the PM2. 5 pollution in Beijing. *Environmental pollution*, *197*, pp.68-75.
12. Choi, K., & Chong, K. (2022). Modified Inverse Distance Weighting Interpolation for Particulate Matter Estimation and Mapping. Atmosphere, 13(5), 846. https://doi.org/10.3390/atmos13050846
13. Danek, T., Weglinska, E. and Zareba, M., 2022. The influence of meteorological factors and terrain on air pollution concentration and migration: a geostatistical case study from Krakow, Poland. *Scientific reports*, *12*(1), p.11050.
14. de Bont, J., Krishna, B., Stafoggia, M., Banerjee, T., Dholakia, H., Garg, A., Ingole, V., Jaganathan, S., Kloog, I., Lane, K. and Mall, R.K., 2024. Ambient air pollution and daily mortality in ten cities of India: a causal modelling study. *The Lancet Planetary Health*, *8*(7), pp.e433-e440.
15. Gandhimathi, A., Manju, R., Ramadevi, K., Rajalakshmi, S. and Mayilvahanan, I., 2023. A study of environmental impact of air pollution on human health: PM deposition modelling. *Global NEST Journal*, *25*(6), pp.35-40.
16. Gupta, P., Satsangi, M., Satsangi, G.P., Jangid, A., Liu, Y., Pani, S.K. and Kumar, R., 2020. Exposure to respirable and fine dust particle over North-Central India: chemical characterization, source

interpretation, and health risk analysis. *Environmental Geochemistry and Health*, *42*(7), pp.2081-2099.

17. Han, L., Zhou, W., Li, W. and Li, L., 2014. Impact of urbanization level on urban air quality: A case of fine particles (PM2. 5) in Chinese cities. *Environmental Pollution*, *194*, pp.163-170.
18. Hossain, M.M., Hassan, M.R. and Miah, M.A., 2023. GIS-based spatial mapping of the atmospheric particulate pollutant (PM2. 5 and PM10) at Mymensingh City corporation areas of Bangladesh. *J. Mater. Environ. Sci*, *14*(9), p.1037.
19. Hsu, W.H., Hwang, S.A., Kinney, P.L. and Lin, S., 2017. Seasonal and temperature modifications of the association between fine particulate air pollution and cardiovascular hospitalization in New York state. *Science of the Total Environment*, *578*, pp.626-632.
20. Ismain, S.H.A., Salleh, S.A., Mohammad Sham, N., Wan Azmi, W.N.F., Zulkiflee, A.L. and Ab Rahman, A.Z., 2023, July. Spatial distribution of particulate matter (PM2. 5) in Klang Valley using inverse distance weighting interpolation model. In *IOP Conference Series: Earth and Environmental Science* (Vol. 1217, No. 1, p. 012033). IOP Publishing.
21. Sharma, S.K. and Mandal, T.K., 2023. Elemental composition and sources of fine particulate matter (PM2. 5) in Delhi, India. *Bulletin of environmental contamination and toxicology*, *110*(3), p.60.
22. Jena, S., Perwez, A. and Singh, G., 2019. Trace element characterization of fine particulate matter and assessment of associated health risk in mining area, transportation routes and institutional area of Dhanbad, India. *Environmental geochemistry and health*, *41*(6), pp.2731-2747.
23. Karagulian, F., Belis, C.A., Dora, C.F.C., Prüss-Ustün, A.M., Bonjour, S., Adair-Rohani, H. and Amann, M., 2015. Contributions to cities' ambient particulate matter (PM): A systematic review of local source contributions at global level. *Atmospheric environment*, *120*, pp.475-483.
24. Khan, S.A., Muhammad, S., Nazir, S. and Shah, F.A., 2020. Heavy metals bounded to particulate matter in the residential and industrial sites of Islamabad, Pakistan: Implications for non-cancer and cancer risks. *Environmental Technology & Innovation*, *19*, p.100822.
25. Khanna, I., Khare, M. and Gargava, P., 2015. Health risks associated with heavy metals in fine particulate matter: a case study in Delhi city, India. *J Geosci Environ Prot*, *3*(02), p.72.
26. Kumari, S., Jain, M.K. and Elumalai, S.P., 2021. Assessment of pollution and health risks of heavy metals in particulate matter and road dust along the road network of Dhanbad, India. *Journal of health & pollution*, *11*(29), p.210305.
27. Lee, S.C., Cheng, Y., Ho, K.F., Cao, J.J., Louie, P.K., Chow, J.C. and Watson, J.G., 2006. PM1. 0 and PM2. 5 characteristics in the roadside environment of Hong Kong. *Aerosol Science and Technology*, *40*(3), pp.157-165.

28. Li, J., Hao, X., Liao, H., Hu, J. and Chen, H., 2021. Meteorological impact on winter PM2. 5 pollution in Delhi: Present and future projection under a warming climate. *Geophysical Research Letters*, *48*(13), p.e2021GL093722.
29. Manisalidis, I., Stavropoulou, E., Stavropoulos, A. and Bezirtzoglou, E., 2020. Environmental and health impacts of air pollution: a review. *Frontiers in public health*, *8*, p.14.
30. Meena, M.D., Dotaniya, M.L., Meena, B.L., Rai, P.K., Antil, R.S., Meena, H.S., Meena, L.K., Dotaniya, C.K., Meena, V.S., Ghosh, A. and Meena, K.N., 2023. Municipal solid waste: Opportunities, challenges and management policies in India: A review. *Waste Management Bulletin*, *1*(1), pp.4-18.
31. Mehta, U.H., Kaul, D.S., Westerdahl, D., Ning, Z., Zhang, K., Sun, L., Wei, P., Gajjar, H.H., Jeyaraman, J.D., Patel, M.V. and Joshi, R.R., 2022. Understanding the sources of heavy metal pollution in ambient air of neighboring a solid waste landfill site. *Aerosol Science and Engineering*, *6*(2), pp.161-175.
32. Mohanraj, R., Azeez, P.A. and Priscilla, T., 2004. Heavy metals in airborne particulate matter of urban Coimbatore. *Archives of environmental contamination and toxicology*, *47*(2), pp.162-167.
33. Murthy, B.S., Latha, R., Tiwari, A., Rathod, A., Singh, S. and Beig, G., 2020. Impact of mixing layer height on air quality in winter. *Journal of Atmospheric and Solar-Terrestrial Physics*, *197*, p.105157.
34. Njoku, P. O., Edokpayi, J. N., & Odiyo, J. O. (2019). Health and Environmental Risks of Residents Living Close to a Landfill: A Case Study of Thohoyandou Landfill, Limpopo Province, South Africa. International Journal of Environmental Research and Public Health, 16(12), 2125. https://doi.org/10.3390/ijerph16122125
35. Nkansah, F.K., Belford, E.J.D., Hogarh, J.N. and Anim, A.K., 2025. Assessment of ambient air quality and health risks from vehicular emissions in urban Ghana: A case study of Winneba. *Journal of Air Pollution and Health*.
36. Palmiotto, M., Fattore, E., Paiano, V., Celeste, G., Colombo, A. and Davoli, E., 2014. Influence of a municipal solid waste landfill in the surrounding environment: Toxicological risk and odor nuisance effects. *Environment international*, *68*, pp.16-24.
37. Patra, A.K., Gorai, A.K., Rengde, V.R. and Sharma, Y., 2021. GIS-based exposure assessment and characterization of particulate matter in a mining region in India: AK Patra et al. *Environment, Development and Sustainability*, *23*(7), pp.9852-9874.
38. Ravindra, K., Singh, T., Mandal, T.K., Sharma, S.K. and Mor, S., 2022. Seasonal variations in carbonaceous species of PM2. 5 aerosols at an urban location situated in Indo-Gangetic Plain and its relationship with transport pathways, including the potential sources. *Journal of environmental management*, *303*, p.114049.

39. Roy, D., Singh, G. and Seo, Y.C., 2019. Carcinogenic and non-carcinogenic risks from PM10-and PM2. 5-Bound metals in a critically polluted coal mining area. *Atmospheric Pollution Research*, *10*(6), pp.1964-1975.
40. Safarov, R., Shomanova, Z., Nossenko, Y., Kopishev, E., Bexeitova, Z. and Kamatov, R., 2024. Spatial analysis of air pollutants in an industrial city using GIS-based techniques: a case study of Pavlodar, Kazakhstan. *Sustainability*, *16*(17), p.7834.
41. Santra, S., 2025. PM2. 5 in India: spatiotemporal trends, source contributions, and health impacts. *Environmental Monitoring and Assessment*, *197*(12), p.1382.
42. Schraufnagel, D.E., 2020. The health effects of ultrafine particles. *Experimental & molecular medicine*, *52*(3), pp.311-317.
43. Govardhan, G., Ghude, S.D., Kumar, R., Sharma, S., Gunwani, P., Jena, C., Yadav, P., Ingle, S., Debnath, S., Pawar, P. and Acharja, P., 2024. Decision Support System version 1.0 (DSS v1. 0) for air quality management in Delhi, India. *Geoscientific Model Development*, *17*(7), pp.2617-2640.
44. Shukla, K., Kumar, P., Mann, G.S. and Khare, M., 2020. Mapping spatial distribution of particulate matter using Kriging and Inverse Distance Weighting at supersites of megacity Delhi. *Sustainable cities and society*, *54*, p.101997.
45. Siudek, P., 2021. Inter-annual variability of trace elements in PM10 and the associated health risk in coastal-urban region (southern Baltic Sea, Poland). *Urban Climate*, *37*, p.100826.
46. Sirithian, D. and Thanatrakolsri, P., 2022. Relationships between meteorological and particulate matter concentrations (PM2. 5 and PM10) during the haze period in urban and rural areas, Northern Thailand. *Air, Soil and Water Research*, *15*, p.11786221221117264.
47. Soumiya, M., Balakrishnan, M. and Shanthi, K., 2018. Composition of municipal solid waste accumulated in vellalore dump yard from Coimbatore city. *Research Journal of life Sciences, Bioinformatics, Pharmaceutical and Chemical sciences*, *4*(4), pp.156-164.
48. Tella, A. and Balogun, A.L., 2022. GIS-based air quality modelling: Spatial prediction of PM10 for Selangor State, Malaysia using machine learning algorithms. *Environmental Science and Pollution Research*, *29*(57), pp.86109-86125.
49. Vallabani, N.S., Gruzieva, O., Elihn, K., Juárez-Facio, A.T., Steimer, S.S., Kuhn, J., Silvergren, S., Portugal, J., Piña, B., Olofsson, U. and Johansson, C., 2023. Toxicity and health effects of ultrafine particles: Towards an understanding of the relative impacts of different transport modes. *Environmental research*, *231*, p.116186.
50. World Health Organization (WHO). (2021). WHO global air quality guidelines. WHO Press, Geneva.

51. Xing, Y.F., Xu, Y.H., Shi, M.H. and Lian, Y.X., 2016. The impact of PM2. 5 on the human respiratory system. *Journal of thoracic disease*, *8*(1), p.E69.
52. Chen, Z., Chen, D., Zhao, C., Kwan, M.P., Cai, J., Zhuang, Y., Zhao, B., Wang, X., Chen, B., Yang, J. and Li, R., 2020. Influence of meteorological conditions on PM2. 5 concentrations across China: A review of methodology and mechanism. *Environment international*, *139*, p.105558.
53. Yang, A.M., Lo, K., Zheng, T.Z., Yang, J.L., Bai, Y.N., Feng, Y.Q., Cheng, N. and Liu, S.M., 2020. Environmental heavy metals and cardiovascular diseases: Status and future direction. *Chronic diseases and translational medicine*, *6*(04), pp.251-259.
54. Zhang, X., Zhou, B., Li, Z., Lin, Y., Li, L., & Han, Y. (2022). Seasonal Distribution of Atmospheric Coarse and Fine Particulate Matter in a Medium-Sized City of Northern China. Toxics, 10(5), 216. https://doi.org/10.3390/toxics10050216
55. Ziernicka-Wojtaszek, A., Zuśka, Z., & Kopcińska, J. (2024). Assessment of the Effect of Meteorological Conditions on the Concentration of Suspended PM2.5 Particulate Matter in Central Europe. Sustainability, 16(11), 4797. https://doi.org/10.3390/su16114797